Found. Comput. Math. 193–225 (2006)

DOI: 10.1007/s10208-004-0122-5

FOUNDATIONS OF COMPUTATIONAL MATHEMATICS
The Journal of the Society for the Foundations of Computational Mathematics

Analysis of a New Nonlinear Subdivision Scheme. Applications in Image Processing

Sergio Amat,[1] Rosa Donat,[2] Jacques Liandrat,[3] and J. Carlos Trillo[4]

[1]Departamento de Matemática Aplicada y Estadística
Universidad Politécnica de Cartagena
Spain
sergio.amat@upct.es

[2]Departament de Matemàtica Aplicada
Universitat de València
Spain
donat@uv.es

[3]Ecole Généraliste d'Ingénieurs de Marseille (EGIM)
Laboratoire d'Analyse Topologie et Probabilites (LATP)
France
liandrat@esm2.imt-mrs.fr

[4]Departamento de Matemática Aplicada y Estadística
Universidad Politécnica de Cartagena
Spain
jc.trillo@upct.es

Abstract. A nonlinear multiresolution scheme within Harten's framework [**12**], [**13**] is presented, based on a new nonlinear, centered piecewise polynomial interpolation technique. Analytical properties of the resulting subdivision scheme, such as convergence, smoothness, and stability, are studied. The stability and the compression properties of the associated multiresolution transform are demonstrated on several numerical experiments on images.

Date received: January 29, 2004. Final version received: February 11, 2005. Date accepted: May 3, 2005. Communicated by Wolfgang Dahmen. Online publication: July 14, 2005.
Key words and phrases: Multiresolution, Nonlinear subdivision scheme, Harmonic mean.
AMS classification: 41A05, 41A10, 65D05, 65D17.

1. Introduction

This paper is devoted to a new nonlinear multiresolution representation scheme for discrete data. Given $f^L = (f_1^L, \ldots, f_j^L, \ldots)$, a data vector where L stands for a resolution level (think, for instance, of a signal f sampled at a frequency 2^L), a multiresolution representation of f^L is a sequence $\{f^0, d^1, \ldots, d^L\}$ where f^k is an approximation of f^L at resolution $k < L$ and d^{k+1} stands for the details required to recover f^{k+1} from f^k. The couple of vectors $\{f^k, d^{k+1}\}$ contains the same information as f^{k+1} and therefore the same is true for $\{f^0, d^1, \ldots, d^L\}$ and f^L. Wavelet decompositions are key examples widely used for image analysis and compression.

It is well known that the efficiency of wavelet decompositions in image compression is generally limited by the presence of discontinuities or edges. On one hand, the numerically significant detail coefficients d_j^k are mainly those for which the associated wavelet support is intersected by such discontinuities. On the other hand, to obtain few significant coefficients in the smooth regions of the signal, highly oscillating wavelets are needed. These wavelets have larger supports, which implies that the number of significant coefficients related to discontinuities is larger.

Harten's framework for multiresolution also provides an adequate setting for the design of discrete multiresolution representations [**12**], [**13**]. Discrete resolution levels are connected by interresolution operators, named decimation (from fine (k) to coarse $(k-1)$) and prediction (from coarse to fine). These interscale operators are directly related to the *discretization* and *reconstruction* operators, which act between the continuous level (where a function f, related to the discrete data, lives) to each discrete level (where f^k lives).

Different settings can be considered depending on the linear discretization operator that produces the data. Classical settings are provided by the sampling operator (point value setting) or the averaging operators (spline settings). Linear multiresolution representations, such as wavelet decompositions, are related to data-independent reconstruction operators, and therefore linear prediction operators (see [**5**], [**6**], [**7**] for more details).

The greatest advantage of Harten's general framework lies in its adaptability. The fundamental role played by the reconstruction operator makes it possible to perform *specific adaptive treatments at singularities*. In general, these involve data-dependent reconstruction operators, which lead to nonlinear prediction schemes and, hence, to nonlinear multiresolution decompositions [**12**], [**13**]. A first step toward nonlinear adaption near singularities has been achieved by Essentially Non Oscillatory (ENO) reconstruction techniques [**12**], [**5**].

A crucial issue in applying nonlinear multiresolution decompositions for image compression is the question of stability. It is shown in [**2**] that *stabilized* ENO multiresolution schemes outperform linear multiresolution schemes of the same order of approximation, based on biorthogonal wavelets, for piecewise smooth geometric images. In [**2**], the authors ensure stability by using the Error Control strategy, originally designed by Harten [**12**]. The Error Control mechanism,

which involves a modification of the direct multiresolution transformation, seems to be essential for the stability of nonlinear ENO multiresolution schemes. It is a known fact that without its application, data compression based on ENO multiresolution schemes can lead to undesirable numerical artifacts (see [**2**] and Section 5).

For simplicity, in this paper we consider the point value setting, where reconstruction is equivalent to interpolation. It is shown in [**5**], [**10**] that data-independent piecewise polynomial interpolation leads to interpolatory wavelets. In the context of image compression, the weakness of piecewise polynomial linear reconstruction techniques appears as a blurring of the image edges.

The ENO interpolation operator takes its roots from the ENO schemes introduced by Harten, Osher, Engquist, and Chakravarthy in [**14**], [**15**] for hyperbolic conservation laws. Following the track opened by Marquina [**17**], Amat, Busquier, and Candela [**3**] introduced the PPH (Piecewise Polynomial Harmonic) method for the interpolation of fluxes in the numerical solution of hyperbolic conservation laws. Making a new step toward nonlinearity, this method is based on a fixed centered stencil together with a specific singularity adaption mechanism that involves a nonlinear interpolation strategy. In the context of conservation laws, the PPH method has been proven to be more efficient than the equivalent (in terms of accuracy) ENO scheme, and simpler to implement than the scheme introduced in [**17**]. The aim of this paper is to describe and analyze the nonlinear multiresolution transform that results from considering the PPH reconstruction technique in Harten's interpolatory setting.

In [**8**], Cohen, Dyn, and Matei developed a general stability approach for the analysis of data-dependent subdivision schemes. The nonlinear prediction operator obtained from the PPH reconstruction does not exactly fit the hypothesis in [**8**] (see Section 4), however we are able to adapt their approach to study the convergence, smoothness, and stability of the subdivision scheme naturally connected to our algorithm.

The paper is organized as follows: In Section 2 we recall the discrete point value framework for multiresolution introduced by Harten [**13**] and its relation with interpolatory subdivision schemes. The PPH reconstruction technique is described in Section 3 and in Section 4 we study the analytical properties of the associated nonlinear subdivision scheme. The compression properties, and related stability issues, of the PPH-based nonlinear multiresolution decomposition are numerically studied in Section 5, including a comparison of its performance with respect to other linear and nonlinear schemes, of the same theoretical accuracy.

2. The Interpolatory Multiresolution Setting

Let us consider a set of nested grids in $\mathbb{R}$:

$$X^k = \{x_j^k\}_{j\in\mathbb{Z}}, \qquad x_j^k = jh_k, \quad h_k = 2^{-k},$$

and the point-value discretization

$$\mathcal{D}_k: \quad \begin{cases} C_B(\mathbb{R}) \to V^k, \\ f \qquad \mapsto f^k = (f_j^k)_{j\in\mathbb{Z}} = (f(x_j^k))_{j\in\mathbb{Z}}, \end{cases} \tag{1}$$

where V^k is the space of real sequences related to the resolution of X^k and $C_B(\mathbb{R})$ the set of bounded continuous functions on $\mathbb{R}$. A reconstruction operator $\mathcal{R}_k$ associated to this discretization is any right inverse of $\mathcal{D}_k$, which means that for all $f^k \in V^k$, $\mathcal{R}_k f^k \in C_B(\mathbb{R})$ and

$$(\mathcal{R}_k f^k)(x_j^k) = f_j^k = f(x_j^k). \tag{2}$$

The sequences $\{\mathcal{D}_k\}$ and $\{\mathcal{R}_k\}$ define a multiresolution transform. The prediction operator, i.e., $\mathcal{D}_{k+1}\mathcal{R}_k$: $V^k \to V^{k+1}$, defines a subdivision scheme. Relation (2) implies that the subdivision scheme is interpolatory (see [**5**] for details). If $\mathcal{R}_k$ is a nonlinear reconstruction operator, the corresponding subdivision scheme is also nonlinear.

2.0.1. *Linear Reconstruction Techniques*: *Data-Independent Lagrange Interpolation*. The standard data-independent Lagrange interpolatory techniques are used to define *linear* reconstruction operators as follows: Given two fixed integers $r \geq 1, s > 0$, $r \geq s$, $(\mathcal{R}_k^{\mathcal{L}} f^k)(x)$ is a piecewise polynomial function defined in each subinterval $[x_j^k, x_{j+1}^k]$ as the unique interpolation polynomial for the data set $\{f_{j+m}^k, m \in \mathcal{S}\}$ with $\mathcal{S} = \mathcal{S}(r,s) = \{-s, -s+1, \ldots, -s+r\}$. The data-independent interpolatory stencil $\mathcal{S}$ completely characterizes $\mathcal{R}_k^{\mathcal{L}}$. The corresponding interpolatory subdivision scheme can be written as a linear filter bank where the coefficients depend solely on the interpolation stencil S (see [**13**]).

Linearity and reproduction of polynomials of degree less than or equal to r implies that for any function $f \in C^{r+1}$, and f^k as in (1),

$$(\mathcal{R}_k^{\mathcal{L}} f^k)(x_{2j+1}^{k+1}) = f(x_{2j+1}^{k+1}) + O(h_k)^{r+1}.$$

The corresponding prediction operator is then said to be of accuracy $p = r + 1$.

Lagrange interpolatory techniques lose their accuracy in the presence of isolated singularities. Indeed, if f has a discontinuity point in $[x_{j-1}^k, x_j^k]$, it is easy to check that any divided difference[1] based on a set of $s+1$ points containing $\{x_{j-1}^k, x_j^k\}$ verifies

$$f[x_l^k, \ldots, x_{l+s}^k] = O([f])/h_k^s, \tag{3}$$

[1] The divided differences are defined by induction as

$$f[x_{i-1}^k, x_i^k] := \frac{f(x_i^k) - f(x_{i-1}^k)}{x_i^k - x_{i-1}^k}$$

and

$$f[x_{i-m}^k, \ldots, x_{i-m+n}^k] := \frac{f[x_{i-m+1}^k, \ldots, x_{i-m+n}] - f[x_{i-m}^k, \ldots, x_{i-m+n-1}^k]}{x_{i-m+n}^k - x_{i-m}^k}.$$

where $[f] = |f_j^k - f_{j-1}^k|$. As a consequence, any Lagrange interpolation polynomial $q(x)$ whose stencil, $\mathcal{S}$, contains both x_{j-1}^k and x_j^k (that is, the stencil *crosses* the jump singularity) satisfies instead

$$f(x) = q(x) + O([f]).$$

This means that the accuracy of the prediction is completely lost on the corresponding interval. More details can be found in [**5**].

2.0.2. *Nonlinear Reconstruction Techniques*: *Data-Dependent ENO Interpolation*. To improve the accuracy of the reconstruction and consequently the efficiency of the corresponding multiresolution transforms, nonlinear techniques are often used. In this section we briefly recall the data-dependent ENO interpolation.

The idea supporting ENO interpolation is to construct polynomial pieces using data belonging to smooth regions of the function, as long as this is possible. The main ingredient is a selection procedure that attempts to choose, for each value of the position parameter j, the stencil $\mathcal{S}$ (i.e., the parameter s) such that the points of interpolation remain within a region of smoothness of the function $f(x)$. Various stencil selection procedures based on divided differences are described in [**15**].

In the presence of isolated singularities, the order of accuracy of an ENO prediction operator constructed from stencils of $r+1$ points remains $r+1$ for all but one prediction interval. For theoretical details and applications, see [**1**], [**2**], [**5**].

One should notice that the stencil selection mechanism implies the use of noncentered stencils. Moreover, investigation of all possible stencils implies that the ENO scheme of order $r+1$ involves $2r$ points for the prediction at each locality, while the linear scheme of the same order only involves $r+1$ points.

3. A New Nonlinear Reconstruction Technique: The PPH Reconstruction

In this section, we describe a fourth-order nonlinear and data-dependent interpolation scheme based on a piecewise polynomial interpolation operator introduced in [**3**] and called PPH interpolation (for Piecewise Polynomial Harmonic).

This nonlinear interpolatory technique leads to a reconstruction operator with several desirable features. First, each polynomial piece is constructed with a fixed centered stencil of four points. Second, the reconstruction is as accurate as its linear equivalent on smooth regions. Third, the accuracy is reduced close to singularities, but it is not completely lost as in its linear counterpart.

Let us describe next the PPH reconstruction operator $\mathcal{R}_k$. Given $x \in \mathbb{R}$, let j be such that $x \in [x_j^k, x_{j+1}^k]$. As with all the other interpolation techniques $(\mathcal{R}_k f^k)(x) = \tilde{P}_j(x, f^k)$. Here $\tilde{P}_j(x, f^k)$ is a polynomial constructed from the centered data f_{j-1}^k, f_j^k, f_{j+1}^k, f_{j+2}^k and such that $\tilde{P}_j(x_j^k, f^k) = f_j^k$ and $\tilde{P}_j(x_{j+1}^k, f^k) = f_{j+1}^k$. In what follows we abbreviate $\tilde{P}_j(x) = \tilde{P}_j(x, f^k)$ and we drop the superindex k for the sake of clarity.

To motivate the definition of $\tilde{P}_j(x)$ we first consider the centered Lagrange interpolatory polynomial $P_j(x)$ of degree 3 defined by the interpolatory conditions

$$P_j(x_m) = f_m, \qquad j-1 \le m \le j+2. \tag{4}$$

Let us write $P_j(x)$ as

$$P_j(x) = a_0 + a_1(x - x_{j+1/2}) + a_2(x - x_{j+1/2})^2 + a_3(x - x_{j+1/2})^3, \tag{5}$$

where $x_{j+1/2} = \frac{1}{2}(x_j + x_{j+1})$.

Then, $P_j(x_{j+1/2}) = a_0$ and $P_j'(x_{j+1/2}) = a_1$. The presence of a singularity in a nearby cell has a dramatic effect on the behavior of the coefficient a_1. It is easy to check that $P_j(x)$ is equivalently defined by

$$\begin{cases} P_j(x_m) = f_m, & j-1 \le m \le j+1, \\ a_1 \quad = \dfrac{f_{j-1} - 27f_j + 27f_{j+1} - f_{j+2}}{24h}, \end{cases} \tag{6}$$

where h is the uniform spacing between the points x_i. We can rewrite the coefficient a_1 introducing the divided differences associated to the interpolatory stencil,

$$e_{j-1/2} = f[x_{j-1}, x_j], \qquad e_{j+1/2} = f[x_j, x_{j+1}], \qquad e_{j+3/2} = f[x_{j+1}, x_{j+2}],$$
$$D_j = f[x_{j-1}, x_j, x_{j+1}], \qquad D_{j+1} = f[x_j, x_{j+1}, x_{j+2}],$$

as

$$a_1 = \frac{-e_{j-1/2} + 13e_{j+1/2}}{12} - \frac{1}{6}\frac{D_j + D_{j+1}}{2}h. \tag{7}$$

For a smooth function, $e_{j-1/2} = O(1)$, $e_{j+1/2} = O(1)$, $D_j = O(1)$, and $D_{j+1} = O(1)$, which leads to $a_1 = O(1)$. Let us suppose now that a discontinuity exists in $[x_{j+1}, x_{j+2}]$, then, because of (3), $D_{j+1} = O(1/h^2)$ and $D_j = O(1)$. Thus, we would obtain $a_1 = O(1/h)$ as a consequence of the presence of a discontinuity in $[x_{j+1}, x_{j+2}]$. We propose to replace a_1 in (7) by the following:

$$\tilde{a}_1 := \frac{-e_{j-1/2} + 13e_{j+1/2}}{12} - \tfrac{1}{6}\tilde{D}h, \tag{8}$$

where

$$\tilde{D} = \begin{cases} \dfrac{2D_jD_{j+1}}{D_j + D_{j+1}} & \text{if } D_jD_{j+1} > 0, \\ 0 & \text{otherwise.} \end{cases} \tag{9}$$

Due to the fact that

$$\left| 2\frac{D_jD_{j+1}}{D_j + D_{j+1}} \right| \le 2\min(|D_j|, |D_{j+1}|) = O(1), \tag{10}$$

we obtain $\tilde{D} = O(1)$, hence $\tilde{a}_1 = O(1)$, instead of $O(1/h)$, as in the linear case.

Then we consider the polynomial

$$\tilde{P}_j(x) = \tilde{a}_0 + \tilde{a}_1(x - x_{j+1/2}) + \tilde{a}_2(x - x_{j+1/2})^2 + \tilde{a}_3(x - x_{j+1/2})^3, \qquad (11)$$

where $\tilde{a}_1$ is given by (8)–(9), and $\tilde{a}_0, \tilde{a}_2, \tilde{a}_3$ are determined by imposing the interpolatory conditions

$$\tilde{P}_j(x_m) = f_m, \qquad j - 1 \le m \le j + 1. \qquad (12)$$

It is easy to check that

$$\tilde{P}_j(x_{j+1/2}) = \frac{f_j + f_{j+1}}{2} - \tfrac{1}{4}\tilde{D}h^2. \qquad (13)$$

It is interesting to compare this expression with the equivalent one obtained from the centered Lagrange interpolatory polynomial $P_j(x)$,

$$P_j(x_{j+1/2}) = \frac{f_j + f_{j+1}}{2} - \frac{1}{4}\frac{D_j + D_{j+1}}{2}h^2. \qquad (14)$$

Comparing (7) to (8) and (13) to (14) we notice that the net effect is the replacement of the arithmetic mean of D_j and D_{j+1} by the "modified" harmonic mean $\tilde{D}$ in (9). The arithmetic mean and the harmonic mean of two values are very close for values of the same magnitude, but the harmonic mean is always bounded in absolute value by twice the absolute value of the smallest of the two numbers. This property is the key to the behavior of the PPH reconstruction close to isolated singularities.

The analysis above leads us to the following definition for the PPH interpolatory reconstruction in the interval $[x_j, x_{j+1}]$. If $|f[x_j, x_{j+1}, x_{j+2}]| \ge |f[x_{j-1}, x_j, x_{j+1}]|$, then $\tilde{P}_j(x)$ is defined by expressions (11)–(12). Otherwise, $|f[x_j, x_{j+1}, x_{j+2}]| < |f[x_{j-1}, x_j, x_{j+1}]|$, $\tilde{P}_j(x)$ is analogously defined by considering now the symmetrical expression of $\tilde{a}_1$,

$$\tilde{a}_1 := \frac{-e_{j+3/2} + 13e_{j+1/2}}{12} + \tfrac{1}{6}\tilde{D}h, \qquad (15)$$

with $\tilde{D}$ defined in (9) and the symmetrical system of interpolatory conditions

$$\tilde{P}_j(x_m) = f_m, \qquad j \le m \le j + 2. \qquad (16)$$

The practical implementation of a PPH-based multiresolution transformation or of a PPH-based subdivision scheme only requires the value of $\tilde{P}_j(x_{j+1/2})$. Due to the symmetry underlying our construction, the value obtained for $\tilde{P}_j(x_{j+1/2})$ is the same when $\tilde{P}_j(x)$ is constructed from (8)–(12) or from (15)–(16). In fact, it is always given by expression (13).

Two reformulations of the proposed modification, derived from elementary algebra, are useful.

Reformulation 1

The modified polynomial used for the prediction at $x_{j+1/2}$ when $|D_j| \leq |D_{j+1}|$ is equivalently defined by

$$\begin{cases} \tilde{P}_j(x_l) & = f_l, \quad \text{for } j-1 \leq l \leq j+1, \\ \tilde{P}_j(x_{j+2}) & = \tilde{f}_{j+2}, \end{cases} \tag{17}$$

with

$$\tilde{f}_{j+2} = f_{j+1} + f_j - f_{j-1} + 4\tilde{D}h^2.$$

When $|D_j| > |D_{j+1}|$ the modified value is $\tilde{f}_{j-1}$ instead.

Reformulation 2

The system of equations (4) can be written as

$$\begin{pmatrix} a_0 \\ a_1 \\ a_2 \\ a_3 \end{pmatrix} = A \begin{pmatrix} f_{j-1} \\ f_j \\ f_{j+1} \\ f_{j+2} \end{pmatrix} \qquad \text{or} \qquad \begin{pmatrix} a_0 \\ a_1 \\ a_2 \\ a_3 \end{pmatrix} = AT_h^{-1} \begin{pmatrix} f_{j-1} \\ f_j \\ f_{j+1} \\ \dfrac{D_j + D_{j+1}}{2} \end{pmatrix},$$

where A^{-1} is the linear operator given by

$$A^{-1} = \begin{pmatrix} 1 & \dfrac{-3h}{2} & \left(\dfrac{-3h}{2}\right)^2 & \left(\dfrac{-3h}{2}\right)^3 \\ 1 & \dfrac{-h}{2} & \left(\dfrac{-h}{2}\right)^2 & \left(\dfrac{-h}{2}\right)^3 \\ 1 & \dfrac{h}{2} & \left(\dfrac{h}{2}\right)^2 & \left(\dfrac{h}{2}\right)^3 \\ 1 & \dfrac{3h}{2} & \left(\dfrac{3h}{2}\right)^2 & \left(\dfrac{3h}{2}\right)^3 \end{pmatrix}$$

and

$$T_h = \begin{pmatrix} 1 & 0 & 0 & 0 \\ 0 & 1 & 0 & 0 \\ 0 & 0 & 1 & 0 \\ \dfrac{1}{(4h^2)} & \dfrac{-1}{(4h^2)} & \dfrac{-1}{(4h^2)} & \dfrac{1}{(4h^2)} \end{pmatrix}$$

and

$$T_h^{-1} = \begin{pmatrix} 1 & 0 & 0 & 0 \\ 0 & 1 & 0 & 0 \\ 0 & 0 & 1 & 0 \\ -1 & 1 & 1 & 4h^2 \end{pmatrix}.$$

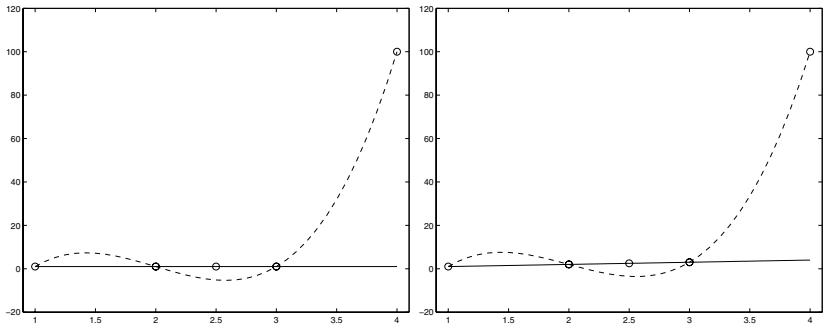

(a) (b)

Fig. 1. o function values: solid line, PPH reconstruction; dashed line, linear reconstruction. (a) $p = 0$ and (b) $p = 1$.

In the case $|D_j| \leq |D_{j+1}|$, $\tilde{P}_j(x)$ is defined by

$$\begin{pmatrix} \tilde{a}_0 \\ \tilde{a}_1 \\ \tilde{a}_2 \\ \tilde{a}_3 \end{pmatrix} = AT_h^{-1} \begin{pmatrix} f_{j-1} \\ f_j \\ f_{j+1} \\ \tilde{D} \end{pmatrix}.$$

When $|D_j| > |D_{j+1}|$ the corresponding rearrangements are done in the first component instead.

To display the behavior of the PPH reconstruction in the presence of isolated discontinuities we consider the functions

$$f(x) = \begin{cases} x^p, & x \leq 3.5, \\ 100, & x \geq 3.5, \end{cases} \qquad p = 0, 1, 2, 3. \tag{18}$$

We consider the stencil of points $\mathcal{S} = \{x_{j-1} = 1, x_j = 2, x_{j+1} = 3, x_{j+2} = 4\}$ and the corresponding function values $\{f_{j+m} = f(x_{j+m})\}_{m=-1}^{2}$. Figures 1 and 2 show the centered Lagrange interpolation polynomial $P_j(x)$ and the PPH polynomial $\tilde{P}_j(x)$ constructed from these data. Their value at $x_{j+1/2} = 2.5$ can be compared to $f(x_{j+1/2})$, marked with a circle as well as $\{f_{j+m}\}$.

As stated in Reformulation 1, we can interpret the PPH reconstruction as Lagrange interpolation where the value at the boundary of the stencil corresponding to a node across a possible discontinuity is modified. As observed in Figures 1 and 2 the net effect is the lack of oscillations.

We establish next some properties of the PPH reconstruction operator:

(1) By construction, the data used for the interpolation remain centered.
(2) The reformulations show that our scheme involves a nonlinear modification of the values f_{j-1} or f_{j+2}, i.e., the values at the boundary of the 4-point stencil.

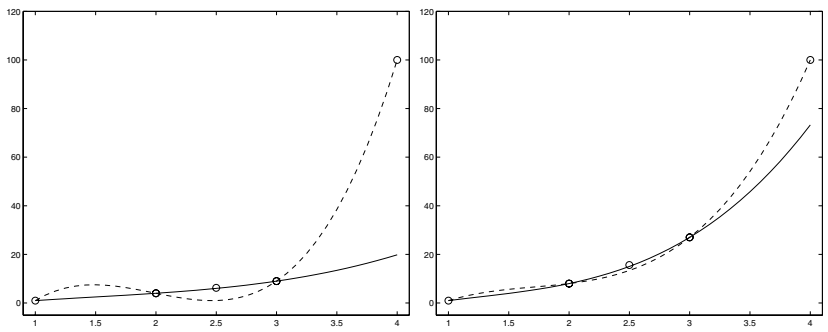

Fig. 2. o function values: solid line, PPH reconstruction; dashed line, linear reconstruction. (a) $p = 2$ and (b) $p = 3$.

(3) If f is a polynomial of degree less than or equal to 2,

$$D_j = D_{j+1} = \frac{D_j + D_{j+1}}{2} = \tilde{D},$$

therefore the proposed scheme reproduces polynomials of degree 2.

(4) If $f \in C^4$ and $D_j D_{j+1} > 0$, using a Taylor expansion we get

$$\begin{aligned} 2\frac{D_j D_{j+1}}{D_j + D_{j+1}} &= \frac{f''(x_{j+1/2})}{2} + O(h^2), \\ \frac{D_j + D_{j+1}}{2} &= \frac{f''(x_{j+1/2})}{2} + O(h^2). \end{aligned}$$

Therefore, in smooth regions, the difference between the arithmetic mean and the harmonic mean is $O(h^2)$.

Using our second reformulation we get that $a_i - \tilde{a}_i = O(h^{4-i})$ for$i = 0, 1, 2, 3$, hence the proposed reconstruction remains fourth-order accurate in smooth regions.

(5) When $D_j D_{j+1} \leq 0$, $\tilde{P}(x_{j+1/2}) = (f_{j+1} + f_j)/2$. In this case, the accuracy of the reconstruction is limited to second order even in smooth regions.

(6) If there is a discontinuity in $[x_{j+1}, x_{j+2}]$ and $D_j D_{j+1} > 0$, due to (10) the Gibbs phenomenon of linear reconstruction does not appear (see Figures 1 and 2). In addition, the order of accuracy of the reconstruction remains $O(h^2)$ in this case.

We have carried out a numerical experiment to check this fact. The function we consider is

$$f(x) = \begin{cases} x^4 & \text{if } x \leq 0.502, \\ x^4 + 10 & \text{otherwise.} \end{cases}$$

Table 1. Approximation errors and numerical order of the PPH reconstruction in the presence of a singularity.

	$2h$	$3h/2$	h
Error	$5.786e-06$	$2.583e-06$	$1.457e-06$
Order		1.987	1.991

We consider three grids with grid sizes $h,\ 3h/2,\ 2h$ for $h = \frac{1}{512}$ represented in the following illustration with vertical lines, triangles, and circles, respectively. We measure the approximation errors committed by the PPH reconstruction in the central interval $\left[\frac{1}{2} - h/2, \frac{1}{2} + h/2\right]$. The singularity at $\mu = 0.502$ is intentionally located so that it belongs to the rightmost interval of the interpolatory stencil used in the PPH reconstruction for each one of the three grids. In Table 1 we compute the approximation errors[2] and the associated numerical orders.

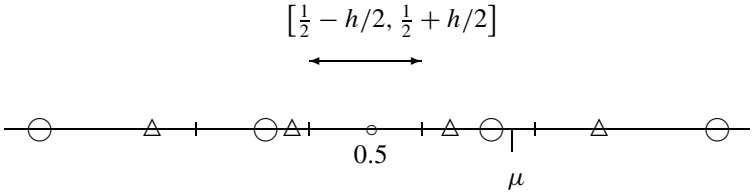

4. The Associated Subdivision Scheme: Convergence, Stability, and Smoothness

As mentioned in Section 2, the prediction operator associated to an interpolatory reconstruction sequence $\{\mathcal{R}_k\}$ defines an interpolatory subdivision scheme. The refinement by subdivision of a sequence at level k is carried out as follows:

$$Sf^k = \mathcal{D}_{k+1}\mathcal{R}_k f^k = \begin{cases} f^{k+1}_{2j+1} = (\mathcal{R}_k f^k)(x^{k+1}_{2j+1}), \\ f^{k+1}_{2j} = (\mathcal{R}_k f^k)(x^{k+1}_{2j}) = f^k_j. \end{cases} \tag{19}$$

Because of the interpolation property, only the odd components of the refined sequence have to be computed. For the PPH reconstruction operator described in the previous section, these can be written as follows:

$$(Sf^k)_{2j+1} = \begin{cases} \dfrac{f_{j+1}+f_j}{2} - \frac{1}{4}\dfrac{D(f)_j D(f)_{j+1}}{D(f)_j + D(f)_{j+1}} & \text{if } D(f)_j D(f)_{j+1} > 0, \\ \dfrac{f_{j+1}+f_j}{2} & \text{else,} \end{cases} \tag{20}$$

[2] We consider a subgrid of 100 points of the interval $\left[\frac{1}{2} - h/2, \frac{1}{2} + h/2\right]$ and measure the errors committed by the reconstruction at these points. The value in Table 1 is the max-norm of the error vector.

with

$$D(f)_i = f_{i+1}^k - 2f_i^k + f_{i-1}^k. \tag{21}$$

Data-independent reconstruction techniques, such as the centered Lagrange interpolation described in the previous section, give rise to *linear* subdivision schemes. The classical definition (see, e.g., [**8**]) is as follows:

Definition 1. A *linear* subdivision operator S is a linear map

$$S\colon l_\infty(\mathbb{Z}) \to l_\infty(\mathbb{Z})$$

defined in terms of a mask $\{a_i\}_{i=-M}^{M}$ so that

$$(Sv)_j := \sum_{l\in\mathbb{Z},|j-2l|\le M} a_{j-2l} v_l.$$

In Harten's framework, ENO interpolatory reconstructions have provided the classical example of nonlinear reconstruction techniques [**5**]. The corresponding subdivision schemes can be interpreted as a nonlinear filter bank, in which we have a finite set of masks of the same length $\{a_k^l\}_{k=-M}^{M}$, $l = 1, \ldots, p$, and one of them is selected, depending on the properties of the data, at each particular location and level [**8**]. The resulting nonlinear subdivision scheme is, clearly, of a different nature from that obtained in (20). The PPH subdivision scheme involves a nonlinear manipulation of the components of the sequence f^k and, therefore, it is intrinsically different from the data-dependent nonlinearity involved in the ENO subdivision schemes. In order to emphasize the difference between *data-dependent* subdivision schemes, as those that are obtained from ENO reconstruction techniques and considered in [**8**], and *fully nonlinear* subdivision schemes, as that obtained from the PPH reconstruction, we propose the following definitions:

Definition 2. [**8**] A data-dependent subdivision operator is an operator valued function that associates to each $f \in l_\infty(\mathbb{Z})$ a linear operator $S(f)\colon l_\infty(\mathbb{Z}) \to l_\infty(\mathbb{Z})$.

Definition 3. A nonlinear subdivision operator is a nonlinear map S: for all $f \in l_\infty(\mathbb{Z}) \mapsto Sf \in l_\infty(\mathbb{Z})$.

In a recent work, Cohen, Dyn, and Matei [**8**] develop a general framework for the analysis of data-dependent subdivision schemes using some extensions of classical results for linear subdivision [**11**]. The fact that $S(f)$ is a linear mapping from $l_\infty(\mathbb{Z})$ into $l_\infty(\mathbb{Z})$ is used to prove that reproduction of polynomials implies the existence of a scheme for the differences. Moreover, they prove that if this scheme satisfies a contraction property the subdivision scheme converges. In addition if the initial scheme is bounded and depends continuously on the data the subdivision scheme is stable.

The subdivision scheme obtained from the repeated application of the PPH prediction operator does not belong to the class analyzed in [**8**]. Given a bounded sequence f, Sf is also a bounded sequence, but it does not make sense to speak of $S(f)$ as a linear mapping. However, the specific form of our scheme makes it possible to follow the main track in [**8**].

We are thus led to introduce some definitions, similar to those in [**8**], but specifically adapted to our nonlinear case.

Definition 4. A nonlinear subdivision operator is called *uniformly convergent* if, for every set of initial data $f^0 \in l_\infty(\mathbb{Z})$, there exists a continuous function $S^\infty f^0 \in C(\mathbb{R})$, such that

$$\lim_{k\to\infty} \|Sf^k - S^\infty f^0(2^{-k}\cdot)\|_{l_\infty(\mathbb{Z})} = 0.$$

Definition 5. A convergent nonlinear subdivision operator is called *stable*, if there exists a constant C such that, for every pair of initial data f^0, $\tilde{f}^0 \in l_\infty(\mathbb{Z})$,

$$\|S^\infty f^0 - S^\infty \tilde{f}^0\|_{L^\infty} \le C\|f^0 - \tilde{f}^0\|_{l_\infty(\mathbb{Z})}.$$

Definition 6. Let $N \ge 0$ be a fixed integer. A nonlinear interpolatory subdivision operator has the property of *polynomial reproduction of order N*, if for all $P \in \prod_N$, $Sp = \tilde{p}$, where p and $\tilde{p}$ are defined by $p_k = P(2^{-k}\cdot)$ and $\tilde{p}_k = P(2^{-(k+1)}\cdot)$.

Definition 7. A nonlinear subdivision operator is called *bounded*, if there exists a constant $C > 0$ such that

$$\|Sf\|_{l_\infty(\mathbb{Z})} \le C\|f\|_{l_\infty(\mathbb{Z})} \quad \text{for all } f \in l_\infty(\mathbb{Z}).$$

Definition 8. A nonlinear subdivision operator is called *Lipschitz continuous* if there exists a constant $C > 0$ such that, for every $f, g \in l_\infty(\mathbb{Z})$, it is verified

$$\|Sf - Sg\|_{l_\infty(\mathbb{Z})} \le C\|f - g\|_{l_\infty(\mathbb{Z})}. \tag{22}$$

We can now prove the following proposition:

Proposition 1. *The nonlinear subdivision operator associated to the PPH reconstruction*:

(1) *reproduces polynomials of degree* $N \le 2$;
(2) *is bounded*; *and*
(3) *is Lipschitz continuous*.

Proof. (1) has been proven in Section 3.

(2) By definition of the PPH subdivision scheme we have

$$(Sf)_{2j} = f_j,$$

$$(Sf)_{2j+1} = \begin{cases} \dfrac{f_{j+1}+f_j}{2} - \frac{1}{4}\dfrac{D(f)_j D(f)_{j+1}}{D(f)_j + D(f)_{j+1}} & \text{if } D(f)_j D(f)_{j+1} > 0, \\ \dfrac{f_{j+1}+f_j}{2} & \text{otherwise.} \end{cases}$$

Using (10) we get that

$$\left| \frac{D(f)_{j+1} D(f)_j}{D(f)_{j+1} + D(f)_j} \right| \le \min(|D(f)_{j+1}|, |D(f)_j|) \le 4\|f\|_{l_\infty(\mathbb{Z})}.$$

Thus,

$$\|Sf\|_{l_\infty(\mathbb{Z})} \le 2\|f\|_{l_\infty(\mathbb{Z})}$$

which proves that the nonlinear subdivision operator is bounded.

(3) Let us consider $\{f\}, \{g\} \in l_\infty(\mathbb{Z})$.

Clearly

$$|(Sf)_{2j} - (Sg)_{2j}| = |f_j - g_j| \le \|f - g\|_{l_\infty(\mathbb{Z})}.$$

Since

$$\left| \frac{f_{j+1}+f_j}{2} - \frac{g_{j+1}+g_j}{2} \right| \le \|f - g\|_{l_\infty(\mathbb{Z})},$$

to estimate the odd components $|(Sf)_{2j+1} - (Sg)_{2j+1}|$ we simply need to estimate the terms

$$\frac{D(f)_{j+1} D(f)_j}{D(f)_{j+1} + D(f)_j}, \qquad \frac{D(g)_{j+1} D(g)_j}{D(g)_{j+1} + D(g)_j},$$

or

$$\frac{D(f)_{j+1} D(f)_j}{D(f)_{j+1} + D(f)_j} - \frac{D(g)_{j+1} D(g)_j}{D(g)_{j+1} + D(g)_j},$$

according to the sign of $D(f)_{j+1} D(f)_j$ and $D(g)_{j+1} D(g)_j$.

(a) Suppose $D(f)_j D(f)_{j+1} > 0$ and $D(g)_j D(g)_{j+1} \le 0$. In particular, $D(f)_{j+1} D(g)_{j+1} \le 0$ or $D(f)_j D(g)_j \le 0$. In the first case, we write

$$\begin{aligned} \left| \frac{D(f)_{j+1} D(f)_j}{D(f)_{j+1} + D(f)_j} \right| &\le \min(|D(f)_{j+1}|, |D(f)_j|) \\ &\le |D(f)_{j+1} - D(g)_{j+1}| \\ &\le 4\|f - g\|_{l_\infty(\mathbb{Z})}, \end{aligned}$$

and in the second case we get similarly

$$\begin{aligned}\left|\frac{D(f)_{j+1}D(f)_j}{D(f)_{j+1}+D(f)_j}\right| &\le \min(|D(f)_{j+1}|, |D(f)_j|)\\ &\le |D(f)_j - D(g)_j|\\ &\le 4\|f-g\|_{l_\infty(\mathbb{Z})}.\end{aligned}$$

(b) Suppose now that $D(f)_j D(f)_{j+1} > 0$ and $D(g)_j D(g)_{j+1} > 0$. If $D(f)_j D(g)_j \le 0$, then using the same arguments as in case (a) we obtain

$$\begin{aligned}&\left|\frac{D(f)_{j+1}D(f)_j}{D(f)_{j+1}+D(f)_j} - \frac{D(g)_{j+1}D(g)_j}{D(g)_{j+1}+D(g)_j}\right|\\ &\qquad\le \left|\frac{D(f)_{j+1}D(f)_j}{D(f)_{j+1}+D(f)_j}\right| + \left|\frac{D(g)_{j+1}D(g)_j}{D(g)_{j+1}+D(g)_j}\right| \le 8\|f-g\|_{l_\infty(\mathbb{Z})}.\end{aligned}$$

If $D(f)_j D(g)_j > 0$, we consider the function $Z(x, y) = xy/(x+y)$ defined for all $xy > 0$. It is easy to check that the Jacobian of the function Z verifies

$$\|J_Z(x, y)\|_\infty \le 1.$$

Thus, the mean value theorem easily leads to

$$\begin{aligned}&\left|\frac{D(f)_{j+1}D(f)_j}{D(f)_{j+1}+D(f)_j} - \frac{D(g)_{j+1}D(g)_j}{D(g)_{j+1}+D(g)_j}\right|\\ &\qquad\le \|(D(f)_{j+1} - D(g)_{j+1}, D(f)_j - D(g)_j)\|_\infty \le 4\|f-g\|_{l_\infty(\mathbb{Z})}.\end{aligned}$$

Clearly, $C = 9$ is a convenient constant that completes the proof for estimate (22) and provides the Lipschitz continuity of the PPH reconstruction. □

In the data-dependent context, it has been proven [**8**] that if the subdivision scheme has the property of reproduction of constants, then there exists a corresponding data-dependent scheme for the differences S_1, such that, given $f^k \in l_\infty(\mathbb{Z})$,

$$S_1(f^k)\colon l_\infty(\mathbb{Z}) \to l_\infty(\mathbb{Z}), \qquad \delta^{k+1} = S_1(f^k)\delta^k,$$

where $\delta_j^k := f_{j+1}^k - f_j^k$. The convergence proof for the data-dependent subdivision schemes in [**8**] is based on the fact that S_1 satisfies a contraction property.

We cannot apply these results directly to our nonlinear subdivision scheme essentially for two reasons. First, the existence of the scheme for differences is not a consequence of reproduction of polynomials because of direct nonlinearity. Second, the *fully nonlinear* character of the scheme.

Here the existence of S_1, as well as a corresponding contraction property have to be proven. We do so in the following proposition:

Proposition 2. *Associated to the PPH nonlinear reconstruction, there exists a nonlinear subdivision scheme S_1 for the differences that satisfies*

$$\|S_1\delta^k\|_{l_\infty(\mathbb{Z})} \le \tfrac{1}{2}\|\delta^k\|_{l_\infty(\mathbb{Z})} \quad \textit{for all } f^k \in l_\infty(\mathbb{Z}),$$

where $\delta_j^k := f_{j+1}^k - f_j^k$.

Proof.

(a) Existence of S_1.

If $D(f^k)_{j+1}D(f^k)_j > 0$,

$$f_{2j+1}^{k+1} = \frac{f_{j+1}^k + f_j^k}{2} - \frac{1}{4}\frac{(f_{j+1}^k - 2f_j^k + f_{j-1}^k)(f_{j+2}^k - 2f_{j+1}^k + f_j^k)}{(f_{j+2}^k - f_{j+1}^k - f_j^k + f_{j-1}^k)}.$$

Then

$$\begin{aligned}
\delta_{(2j+1)}^{k+1} &= f_{2j+2}^{k+1} - f_{2j+1}^{k+1} \\
&= f_{j+1}^k - \frac{f_{j+1}^k + f_j^k}{2} + \frac{1}{4}\frac{(f_{j+1}^k - 2f_j^k + f_{j-1}^k)(f_{j+2}^k - 2f_{j+1}^k + f_j^k)}{(f_{j+2}^k - f_{j+1}^k - f_j^k + f_{j-1}^k)} \\
&= \frac{(\delta_{j+1}^k - \delta_{j-1}^k)\delta_j^k + 2\delta_{j+1}^k\delta_j^k - (\delta_j^k)^2 - \delta_{j+1}^k\delta_{j-1}^k}{4(\delta_{j+1}^k - \delta_{j-1}^k)} \\
&= \tfrac{1}{4}\delta_{j+1}^k \frac{1}{1 + \dfrac{\delta_{j+1}^k - \delta_j^k}{\delta_j^k - \delta_{j-1}^k}} + \tfrac{1}{4}\delta_j^k \left(1 + \frac{1}{1 + \dfrac{\delta_j^k - \delta_{j-1}^k}{\delta_{j+1}^k - \delta_j^k}}\right).
\end{aligned}$$

Otherwise,

$$f_{2j+1}^{k+1} = \frac{f_{j+1}^k + f_j^k}{2}, \tag{23}$$

and then

$$\delta_{(2j+1)}^{k+1} = f_{2j+2}^{k+1} - f_{2j+1}^{k+1} = f_{j+1}^k - \frac{f_{j+1}^k + f_j^k}{2} = \frac{\delta_j^k}{2}.$$

Since $D(f^k)_{j+1}D(f^k)_j = (\delta_{j+1}^k - \delta_j^k)(\delta_j^k - \delta_{j-1}^k) > 0$ we can write

$$(S_1\delta^k)_{2j+1} =$$

$$\begin{cases}
\tfrac{1}{4}\delta_{j+1}^k \dfrac{1}{1+\dfrac{\delta_{j+1}^k - \delta_j^k}{\delta_j^k - \delta_{j-1}^k}} + \tfrac{1}{4}\delta_j^k \left(1 + \dfrac{1}{1+\dfrac{\delta_j^k - \delta_{j-1}^k}{\delta_{j+1}^k - \delta_j^k}}\right) & \text{if } (\delta_{j+1}^k - \delta_j^k)(\delta_j^k - \delta_{j-1}^k) > 0, \\
\dfrac{\delta_j^k}{2} & \text{otherwise.}
\end{cases}$$

Similarly, we get for the even indexes,

$$(S_1\delta^k)_{2j} =$$

$$\begin{cases} \frac{1}{4}\delta^k_{j-1}\dfrac{1}{1+\dfrac{\delta^k_j-\delta^k_{j-1}}{\delta^k_{j+1}-\delta^k_j}}+\frac{1}{4}\delta^k_j\left(1+\dfrac{1}{1+\dfrac{\delta^k_{j+1}-\delta^k_j}{\delta^k_j-\delta^k_{j-1}}}\right) & \text{if } (\delta^k_{j+1}-\delta^k_j)(\delta^k_j-\delta^k_{j-1})>0, \\ \dfrac{\delta^k_j}{2} & \text{else.} \end{cases}$$

Note that S_1 is also a nonlinear scheme, according to Definition 3.

(b) Contraction property.

It follows from the fact that when $(\delta^k_{j+1}-\delta^k_j)(\delta^k_j-\delta^k_{j-1})>0$,

$$\left|\frac{1}{1+\dfrac{\delta^k_{j+1}-\delta^k_j}{\delta^k_j-\delta^k_{j-1}}}\right|+\left|\frac{1}{1+\dfrac{\delta^k_j-\delta^k_{j-1}}{\delta^k_{j+1}-\delta^k_j}}\right|=\frac{1}{1+\dfrac{\delta^k_{j+1}-\delta^k_j}{\delta^k_j-\delta^k_{j-1}}}+\frac{1}{1+\dfrac{\delta^k_j-\delta^k_{j-1}}{\delta^k_{j+1}-\delta^k_j}}=1,$$

and from (23). Then, for all $f^k \in l_\infty(\mathbb{Z})$,

$$\|S_1\delta^k\|_{l_\infty(\mathbb{Z})} \le \tfrac{1}{2}\|\delta^k\|_{l_\infty(\mathbb{Z})}. \tag{24}$$

□

As in [**8**] we now use these results to prove the convergence of the PPH scheme and the smoothness of the limit function. First we prove two lemmas that we will need later.

Lemma 1. *Let $\{\mathcal{R}_k\}$ be the sequence of nonlinear PPH reconstruction operators and S the PPH interpolatory subdivision scheme. There exists C such that, if $f^{k+1} = Sf^k$, then for all k,*

$$\|\mathcal{R}_{k+1}(f^{k+1}) - \mathcal{R}_k(f^k)\|_{L^\infty} \le C\|\delta^k\|_{l_\infty(\mathbb{Z})}, \tag{25}$$

where $\delta^k_j = f^k_{j+1} - f^k_j$.

Proof. Let $f^k \in l_\infty(\mathbb{Z})$, and $x \in \mathbb{R}$. Let j be such that $x \in [x^k_j, x^k_{j+1}]$, and assume that $x \in [x^{k+1}_{2j}, x^{k+1}_{2j+1}]$ (the case $x \in [x^{k+1}_{2j+1}, x^{k+1}_{2j+2}]$ is similar).

We can write

$$\begin{aligned} |\mathcal{R}_{k+1}(f^{k+1})(x) - \mathcal{R}_k(f^k)(x)| \le\ & |\mathcal{R}_{k+1}(f^{k+1})(x) - \mathcal{R}^{\mathcal{L}}_{k+1}(f^{k+1})(x)| \\ & + |\mathcal{R}^{\mathcal{L}}_{k+1}(f^{k+1})(x) - \mathcal{R}^{\mathcal{L}}_k(f^k)(x)| \\ & + |\mathcal{R}^{\mathcal{L}}_k(f^k)(x) - \mathcal{R}_k(f^k)(x)|, \end{aligned}$$

where $\mathcal{R}_k^{\mathcal{L}}$ stands for the centered Lagrange reconstruction operators of the same order.

(1) We prove the bound first for the second term on the right-hand side. Since $x \in [x_{2j}^{k+1}, x_{2j+1}^{k+1}] \subset [x_j^k, x_{j+1}^k]$ we can write

$$R_{k+1}^{\mathcal{L}}(f^{k+1})(x) = \sum_{m=-1}^{2} A_m(x) f_{2j+m}^{k+1},$$

$$\mathcal{R}_k^{\mathcal{L}}(f^k)(x) = \sum_{m=-1}^{2} B_m(x) f_{j+m}^k,$$

with $A_m(x) = L_m((x - x_{2j}^{k+1})/h_{k+1})$ and $B_m(x) = L_m((x - x_j^k)/h_k)$. Here $L_m(x), m = -1, 0, 1, 2$ are the Lagrange basis for the 4-point centered interpolatory stencil.[3] Since $(x - x_{2j}^{k+1})/h_{k+1} \in [0, 1]$ and $(x - x_j^k)/h_k \in [0, 1]$, then

$$|A_m(x)| < 1, \qquad |B_m(x)| < 1. \tag{26}$$

From now on, we drop the explicit dependence on x for the sake of clarity and write simply A_m and B_m when referring to these quantities.

Since $f^{k+1} = Sf^k$, and S is interpolatory, we have

$$\begin{aligned} |\mathcal{R}_{k+1}^{\mathcal{L}}(f^{k+1})(x) - \mathcal{R}_k^{\mathcal{L}}(f^k)(x)| = {} & |A_{-1} f_{2j-1}^{k+1} - B_{-1} f_{j-1}^k \\ & + (A_0 - B_0) f_j^k + A_1 f_{2j+1}^{k+1} \\ & + (A_2 - B_1) f_{j+1}^k - B_2 f_{j+2}^k|, \end{aligned}$$

with

$$f_{2j-1}^{k+1} = \begin{cases} \dfrac{f_{j-1}^k + f_j^k}{2} - \dfrac{1}{4} \dfrac{(\delta_{j-1}^k - \delta_{j-2}^k)(\delta_j^k - \delta_{j-1}^k)}{\delta_j^k - \delta_{j-2}^k} & \text{or} \\ \dfrac{f_{j-1}^k + f_j^k}{2}, \end{cases}$$

and

$$f_{2j+1}^{k+1} = \begin{cases} \dfrac{f_{j+1}^k + f_j^k}{2} - \dfrac{1}{4} \dfrac{(\delta_j^k - \delta_{j-1}^k)(\delta_{j+1}^k - \delta_j^k)}{\delta_{j+1}^k - \delta_{j-1}^k}, & \text{or} \\ \dfrac{f_{j-1}^k + f_j^k}{2}. \end{cases}$$

Hence, we have to analyze four different possibilities. Taking into account the properties of the harmonic mean

$$\left| \frac{(\delta_{j-1}^k - \delta_{j-2}^k)(\delta_j^k - \delta_{j-1}^k)}{\delta_j^k - \delta_{j-2}^k} \right| \leq 2 \|\delta^k\|_{l_\infty(\mathbb{Z})}, \tag{27}$$

[3] $L_m(y) = \prod_{l=-1, l\neq m}^{2} ((y - l)/(m - l))$.

and similarly for the corresponding term in f_{2j+1}^{k+1}, it is sufficient to consider only the simplest case, that is,

$$|\mathcal{R}_{k+1}^{\mathcal{L}}(f^{k+1})(x) - \mathcal{R}_k^{\mathcal{L}}(f^k)(x)| = \left| A_{-1}\left(\frac{f_{j-1}^k + f_j^k}{2}\right) - B_{-1} f_{j-1}^k + (A_0 - B_0) f_j^k + A_1\left(\frac{f_{j+1}^k + f_j^k}{2}\right) + (A_2 - B_1) f_{j+1}^k - B_2 f_{j+2}^k \right|.$$

The right-hand side can be rewritten as

$$\left| \left(\frac{A_{-1}}{2} - B_{-1}\right)(f_{j-1}^k - f_j^k) + \left(A_{-1} - B_{-1} + A_0 - B_0 + \frac{A_1}{2}\right)(f_j^k - f_{j+1}^k) + B_2(f_{j+1}^k - f_{j+2}^k) \right|.$$

Then, using (26),

$$|\mathcal{R}_{k+1}^{\mathcal{L}}(f^{k+1})(x) - \mathcal{R}_k^{\mathcal{L}}(f^k)(x)| \le C_1 \|\delta^k\|_{l_\infty(\mathbb{Z})}. \tag{28}$$

(2) Let us estimate now $|\mathcal{R}_k^{\mathcal{L}}(f^k)(x) - \mathcal{R}_k(f^k)(x)|$.
Using Reformulation 1, we have

$$\mathcal{R}_k(f^k)(x) = \begin{cases} B_{-1} f_{j-1}^k + B_0 f_j^k + B_1 f_{j+1}^k + B_2 \tilde{f}_{j+2}^k & \text{or} \\ B_{-1} \tilde{f}_{j-1}^k + B_0 f_j^k + B_1 f_{j+1}^k + B_2 f_{j+2}^k, \end{cases}$$

depending on the relative sizes of $D(f^k)_j$ and $D(f^k)_{j+1}$. Let us suppose, without loss of generality, that we are in the first case, then

$$|\mathcal{R}_k^{\mathcal{L}}(f^k)(x) - \mathcal{R}_k(f^k)(x)| \le |B_2(f_{j+2}^k - \tilde{f}_{j+2}^k)|. \tag{29}$$

We have two possible cases

$$\tilde{f}_{j+2}^k = \begin{cases} f_{j+1}^k + f_j^k - f_{j-1}^k & \text{or} \\ f_{j+1}^k + f_j^k - f_{j-1}^k + 4\dfrac{(\delta_j^k - \delta_{j-1}^k)(\delta_{j+1}^k - \delta_j^k)}{\delta_{j+1}^k - \delta_{j-1}^k}. \end{cases}$$

In the first one,

$$|f_{j+2}^k - \tilde{f}_{j+2}^k| \le |\delta_{j+1}^k| + |\delta_{j-1}^k| \le 2\|\delta^k\|_{l_\infty(\mathbb{Z})}, \tag{30}$$

and, in the second, using (27),

$$|f^k_{j+2} - \tilde{f}^k_{j+2}| \le 2\|\delta^k\|_{l_\infty(\mathbb{Z})} + 4\left|\frac{(\delta^k_j - \delta^k_{j-1})(\delta^k_{j+1} - \delta^k_j)}{\delta^k_{j+1} - \delta^k_{j-1}}\right| \le 10\|\delta^k\|_{l_\infty(\mathbb{Z})}. \tag{31}$$

Therefore, we have

$$|\mathcal{R}^{\mathcal{L}}_k(f^k)(x) - \mathcal{R}_k(f^k)(x)| \le C_2\|\delta^k\|_{l_\infty(\mathbb{Z})}. \tag{32}$$

(3) Finally, using the previous estimate and Proposition 2, we get that

$$|\mathcal{R}_{k+1}(f^{k+1})(x) - \mathcal{R}^{\mathcal{L}}_{k+1}(f^{k+1})(x)| \le C_2\|\delta^{k+1}\|_{l_\infty(\mathbb{Z})} \le \frac{C_2}{2}\|\delta^k\|_{l_\infty(\mathbb{Z})}, \tag{33}$$

which completes the proof. □

Lemma 2. *The interpolatory PPH reconstruction operators $\mathcal{R}_k$ have the following properties*:

(1) $\|\mathcal{R}_k f^k\|_{L^\infty} \le C\|f^k\|_{l_\infty(\mathbb{Z})}$ *for all* k;
(2) *for each level* k, *for all* x, y *such that* $2^{-k} < |x - y| < 2^{-(k-1)}$, *there exists a constant* C *such that*

$$|\mathcal{R}_k(f^k)(x) - \mathcal{R}_k(f^k)(y)| \le C\|\delta^k\|_{l_\infty(\mathbb{Z})}. \tag{34}$$

Proof. (1) Let $f^k \in l_\infty(\mathbb{Z})$, and $x \in \mathbb{R}$. Consider j such that $x \in [x^k_j, x^k_{j+1}]$. Depending on the relative sizes of $D(f^k)_j$ and $D(f^k)_{j+1}$ we have

$$\mathcal{R}_k(f^k)(x) = \begin{cases} B_{-1}f^k_{j-1} + B_0 f^k_j + B_1 f^k_{j+1} + B_2\tilde{f}^k_{j+2} & \text{or} \\ B_{-1}\tilde{f}^k_{j-1} + B_0 f^k_j + B_1 f^k_{j+1} + B_2 f^k_{j+2}, \end{cases}$$

where B_{-1}, B_0, B_1, B_2 are as defined in Lemma 1. Let us suppose, without loss of generality, that we are in the first case, then

$$|\mathcal{R}_k(f^k)(x)| \le (|B_{-1}| + |B_0| + |B_1|)\,\|f^k\|_{l_\infty} + |B_2|\,|\tilde{f}^k_{j+2}|.$$

Since

$$\tilde{f}^k_{j+2} = \begin{cases} f^k_{j+1} + f^k_j - f^k_{j-1} & \text{or} \\ f^k_{j+1} + f^k_j - f^k_{j-1} + 4\dfrac{(\delta^k_j - \delta^k_{j-1})(\delta^k_{j+1} - \delta^k_j)}{\delta^k_{j+1} - \delta^k_{j-1}}, \end{cases}$$

we easily get, using the property of the harmonic mean in (27),

$$|\tilde{f}^k_{j+2}| \le 19\|f^k\|_{l_\infty}.$$

Since $|B_i| \le 1$, $i = -1, 0, 1, 2$, as stated in (26), we readily obtain

$$|\mathcal{R}_k(f^k)(x)| \le 22\|f^k\|_{l_\infty}.$$

We now prove property (2). We write

$$\begin{aligned}|\mathcal{R}_k(f^k)(x) - \mathcal{R}_k(f^k)(y)| \;\le\; & |\mathcal{R}_k(f^k)(x) - \mathcal{R}_k^{\mathcal{L}}(f^k)(x)| \\ & + |\mathcal{R}_k^{\mathcal{L}}(f^k)(x) - \mathcal{R}_k^{\mathcal{L}}(f^k)(y)| \\ & + |\mathcal{R}_k^{\mathcal{L}}(f^k)(y) - \mathcal{R}_k(f^k)(y)|.\end{aligned}$$

In Lemma 1 we proved that

$$|\mathcal{R}_k^{\mathcal{L}}(f^k)(x) - \mathcal{R}_k(f^k)(x)| \le C_1 \|\delta^k\|_{l_\infty(\mathbb{Z})} \quad \text{for all } x \in \mathbb{R}. \tag{35}$$

Then, we focus now on the second term. Let us suppose $x \in [x_j^k, x_{j+1}^k]$, then $y \in [x_s^k, x_{s+1}^k]$ with $|s - j| \le 2$. We write

$$\begin{aligned}\mathcal{R}_k^{\mathcal{L}}(f^k)(x) \;&=\; B_{-1} f_{j-1}^k + B_0 f_j^k + B_1 f_{j+1}^k + B_2 f_{j+2}^k, \\ \mathcal{R}_k^{\mathcal{L}}(f^k)(y) \;&=\; D_{-1} f_{s-1}^k + D_0 f_s^k + D_1 f_{s+1}^k + D_2 f_{s+2}^k.\end{aligned}$$

Then

$$\begin{aligned}|\mathcal{R}_k^{\mathcal{L}}(f^k)(x) - \mathcal{R}_k^{\mathcal{L}}(f^k)(y)| \;=\; & |B_{-1} f_{j-1}^k + B_0 f_j^k + B_1 f_{j+1}^k + B_2 f_{j+2}^k \\ & - D_{-1} f_{s-1}^k - D_0 f_s^k - D_1 f_{s+1}^k - D_2 f_{s+2}^k|.\end{aligned}$$

Regrouping terms,

$$\begin{aligned}|\mathcal{R}_k^{\mathcal{L}}(f^k)(x) - \mathcal{R}_k^{\mathcal{L}}(f^k)(y)| \;=\; & |B_{-1}(f_{j-1}^k - f_{s-1}^k) + B_0(f_j^k - f_s^k) \\ & + B_1(f_{j+1}^k - f_{s+1}^k) + B_2(f_{j+2}^k - f_{s+2}^k) \\ & + (B_{-1} - D_{-1}) f_{s-1}^k + (B_0 - D_0) f_s^k \\ & + (B_1 - D_1) f_{s+1}^k + (B_2 - D_2) f_{s+2}^k|.\end{aligned}$$

Since $B_{-1} + B_0 + B_1 + B_2 = D_{-1} + D_0 + D_1 + D_2 = 1$, we can plug f_s^k into the previous formula as follows:

$$\begin{aligned}|\mathcal{R}_k^{\mathcal{L}}(f^k)(x) - \mathcal{R}_k^{\mathcal{L}}(f^k)(y)| \;\le\; & |B_{-1}(f_{j-1}^k - f_{s-1}^k) + B_0(f_j^k - f_s^k) \\ & + B_1(f_{j+1}^k - f_{s+1}^k) + B_2(f_{j+2}^k - f_{s+2}^k) \\ & + |(B_{-1} - D_{-1})(f_{s-1}^k - f_s^k) \\ & + (B_1 - D_1)(f_{s+1}^k - f_s^k) \\ & + (B_2 - D_2)(f_{s+2}^k - f_s^k)|.\end{aligned}$$

Now taking into account that $|B_i| \le 1$, $|D_i| \le 1$, $i = -1, 0, 1, 2$, and that $|s - j| \le 2$, we get

$$\begin{aligned}|\mathcal{R}_k^{\mathcal{L}}(f^k)(x) - \mathcal{R}_k^{\mathcal{L}}(f^k)(y)| \;\le\; & (4|s - j| + |B_{-1} - D_{-1}| + |B_1 - D_1| \\ & + 2|B_2 - D_2|)\|\delta^k\|_{l_\infty(\mathbb{Z})} \le 16\|\delta^k\|_{l_\infty(\mathbb{Z})}. \quad \square\end{aligned}$$

The following proposition uses standard arguments to prove the convergence of the nonlinear PPH subdivision scheme. The limit function turns out to be Hölder continuous with exponent $\alpha = 1$.

Proposition 3. *The nonlinear subdivision scheme associated to the PPH reconstruction is uniformly convergent. Moreover, for any $f \in l_\infty(\mathbb{Z})$, the limit function $\mathcal{S}^\infty(f)$ satisfies*

there exists C such that for all $x, y \in \mathbb{R}$, $\quad |S^\infty(f)(x) - S^\infty(f)(y)| \leq C|x-y|.$

Proof. Let $f^0 = f \in l_\infty(\mathbb{Z})$. From (24) we get that

$$\|\delta^k\|_{l_\infty(\mathbb{Z})} \leq (\tfrac{1}{2})^k \|\delta^0\|_{l_\infty(\mathbb{Z})}, \tag{36}$$

On the other hand, from Lemma 1, given the interpolatory PPH reconstruction operators $\mathcal{R}_k$ for each level k, we have

$$\|\mathcal{R}_{k+1}(f^{k+1}) - \mathcal{R}_k(f^k)\|_{L^\infty} \leq C_1 \|\delta^k\|_{l_\infty(\mathbb{Z})}. \tag{37}$$

The property (37) together with (36) imply that $\mathcal{R}_k(f^k)$ is a Cauchy sequence in $C_B(\mathbb{R})$, the space of continuous and bounded functions in $\mathbb{R}$. Since $C_B(\mathbb{R})$ equipped with the L^∞ norm is a Banach space, there exist $\mathcal{S}^\infty(f) = \lim_{k\to\infty} \mathcal{R}_k(f^k)$.

In order to prove the smoothness of the limit function we have that

$$|\mathcal{S}^\infty(f)(x) - \mathcal{R}_k(f^k)(x)| \leq \sum_{l\geq k} |\mathcal{R}_{l+1}(f^{l+1})(x) - \mathcal{R}_l(f^l)(x)|.$$

Using (36) and (37) we get

$$|\mathcal{S}^\infty(f)(x) - \mathcal{R}_k(f^k)(x)| \leq C_2 \|\delta^k\|_{l_\infty(\mathbb{Z})}. \tag{38}$$

If $2^{-k} < |x - y| < 2^{-(k-1)}$, from Lemma 2 we obtain

$$|\mathcal{R}_k(f^k)(x) - \mathcal{R}_k(f^k)(y)| \leq C_3 \|\delta^k\|_{l_\infty(\mathbb{Z})}, \tag{39}$$

and therefore

$$|\mathcal{S}^\infty(f)(x) - \mathcal{S}^\infty(f)(y)| \leq (2C_2 + C_3)\|\delta^k\|_{l_\infty(\mathbb{Z})}.$$

Then, from (36),

$$|\mathcal{S}^\infty(f)(x) - \mathcal{S}^\infty(f)(y)| \leq (2C_2 + C_3)\left(\tfrac{1}{2}\right)^k \|\delta^0\|_{l_\infty(\mathbb{Z})}.$$

We deduce

$$|\mathcal{S}^\infty(f)(x) - \mathcal{S}^\infty(f)(y)| \leq C|x - y|,$$

with $C = (2C_2+C_3)\|\delta^0\|_{l_\infty(\mathbb{Z})}$, that is, the limit function $S^\infty(f)$ satisfies a Lipschitz condition, which completes the proof. □

The specific form of the PPH scheme, in terms of $D(f)_i$, makes it easier to prove stability by working a contraction property for the second differences, instead of the first ones as in [**8**]. While this paper was being reviewed, we proved the following two-step contraction property [**4**]:

Proposition 4. *Denoting* $\hat{f} = S(f)$, $\hat{g} = S(g)$, $\bar{f} = S(\hat{f})$, *and* $\bar{g} = S(\hat{g})$, *then the following inequality holds*:

$$\text{(1)} \qquad \|D(\hat{f})\|_{l_\infty(\mathbb{Z})} \leq \tfrac{1}{2}\|D(f)\|_{l_\infty(\mathbb{Z})},$$

$$\text{(2)} \qquad |D(\hat{f}-\hat{g})_j| \leq \tfrac{1}{2}\|D(f-g)\|_{l_\infty(\mathbb{Z})}, \quad \textit{for } j = 2n+1,$$

$$|D(\hat{f}-\hat{g})_j| \leq \|D(f-g)\|_{l_\infty(\mathbb{Z})}, \quad \textit{for } j = 2n, \tag{40}$$

and

$$\text{(3)} \qquad \|D(\bar{f}-\bar{g})\|_{l_\infty(\mathbb{Z})} \leq \tfrac{3}{4}\|D(f-g)\|_{l_\infty(\mathbb{Z})}.$$

A direct consequence, that ensures the stability of the PPH subdivision scheme, is also proven in [**4**], and reads

Proposition 5 (Stability of the PPH Subdivision Scheme). *Given* $f, \tilde{f} \in l_\infty$, *we have*

$$\|\mathcal{S}^\infty(f) - \mathcal{S}^\infty(\tilde{f})\|_{L^\infty} \leq 9\|f-\tilde{f}\|_{l_\infty(\mathbb{Z})}. \tag{41}$$

Remark 1. The results in Propositions 4 and 5 and similar results involving, moreover, the details of the multiresolution, are the basis for the proof of the stability of the associated PPH multiresolution scheme in [**4**]. Thus, even though not in the same sense as in the linear case, the stability of the subdivision scheme turns out to be a key point to prove the stability of the associated multiresolution scheme.

5. Numerical Experiments

In using nonlinear reconstruction operators for data compression purposes, stability with respect to perturbations is a main issue. Understanding the stability and smoothness of the subdivision algorithms is fundamental in the context of *linear* multiscale transformations. The role played by the subdivision scheme in the stability of nonlinear multiresolution transforms is more subtle. It has now been proven that the nonlinear PPH multiresolution transform is a stable algorithm [**4**].

The goal of this section is to illustrate the compression properties and the general performance of the PPH multiresolution algorithm by comparing it to two other multiresolution algorithms based on fourth-order accurate prediction operators: the

centered 4-point Lagrange interpolatory reconstruction $\mathcal{R}_k^{\mathcal{L}}$ (i.e., the 4-point linear Delauries and Dubuc interpolatory wavelet transform [**9**], [**10**]) and the 4-point data-dependent ENO reconstruction [**5**], [**2**] (notice that six points are involved in the stencil selection process for the fourth-order ENO reconstruction).

We apply the one-dimensional transforms to images via the classical two dimensional tensor product approach [**16**] to generate the two-dimensional multiresolution algorithm. At each level, three sets of details (Δ_1^k, Δ_2^k, and Δ_3^k) are required to recover the approximation A^k from its decimated version A^{k-1}. The classical representation [**16**] is

$$A^k \longleftrightarrow \left(\begin{array}{c|c} A^{k-1} & \Delta_2^k \\ \hline \Delta_3^k & \Delta_1^k \end{array}\right). \tag{42}$$

In the numerical tests J_L refers to the number of pixels in the image ($J_L \times J_L$). The multiresolution transform is applied L times, producing A^0, a coarse image of dimension $J_0 \times J_0$, such that $J_L/J_0 = 2^L$, and Δ, a sequence of details.

For the sake of notation, the two-dimensional multiresolution algorithms based on the linear, ENO, and PPH reconstruction operators will be denoted as LIN4, ENO4, and PPH, respectively.

Due to the finite dimension of images, a special treatment at the boundaries is required. The one-dimensional boundary treatment involves a modification of one predicted value next to the boundary at each level. In the one-dimensional transform the treatment at the left boundary is as follows:

$$(P_{k-1}^k f^{k-1})_1 = \left(\tfrac{5}{16} f_0^{k-1} + \tfrac{15}{16} f_1^{k-1} - \tfrac{5}{16} f_2^{k-1} + \tfrac{1}{16} f_3^{k-1}\right).$$

The symmetric expression is applied at the right boundary. This modification is implemented in all three cases.

To analyze the compression properties we introduce ε, a truncation parameter, and the truncation operator $\mathbf{tr}^{\varepsilon}$ defined as

$$\mathbf{tr}^{\varepsilon}(A^0, \Delta) = (A^0, \hat{\Delta}),$$

with

$$(\hat{\Delta}_l^k)_{ij} = \begin{cases} 0, & |(\Delta_l^k)_{ij}| \le \varepsilon, \\ (\Delta_l^k)_{ij}, & \text{otherwise.} \end{cases}$$

The same value of ε is used for all multiresolution levels.

After truncation, the inverse multiresolution transform is applied to obtain

$$\hat{A}^L = M^{-1}\, \mathbf{tr}^{\varepsilon}(M A^L),$$

which is then compared to the original image using the following norms:

$$\|A^L - \hat{A}^L\|_{l_p} = \left(\frac{1}{(J_L+1)^2} \sum_i |A_i^L - \hat{A}_i^L|^p\right)^{1/p}, \qquad p = 1, 2,$$

$$\|A^L - \hat{A}^L\|_{l_\infty} = \max_i (|A_i^L - \hat{A}_i^L|).$$

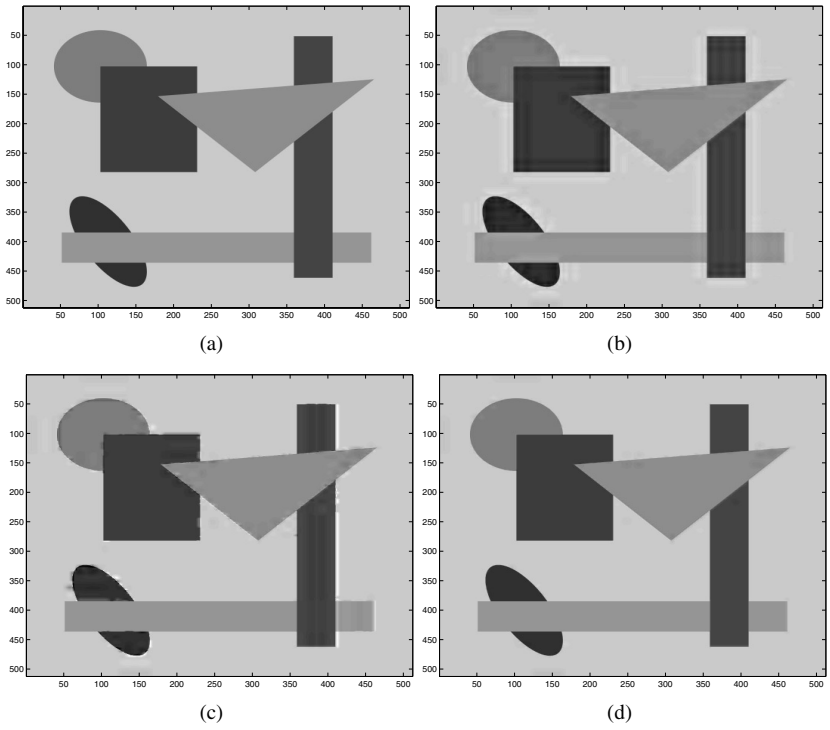

Fig. 3. (a) Geometric image, (b) LIN4, (c) ENO4, and (d) PPH, $L = 4$, $\varepsilon = 10$.

The compression ratio is defined as in [**12**], [**13**] by

$$r_c = \frac{nnz}{(J_L + 1) \times (J_L + 1) - (J_0 + 1) \times (J_0 + 1)},$$

where nnz denotes the number of nonzero detail coefficients. Note that the smaller r_c, the larger the compression achieved.

We consider first the geometric image displayed in Figure 3(a), which is composed of different geometrical objects of constant luminosity. We apply the three algorithms to this image with $L = 4$ and $\varepsilon = 10$, and display the results in Figure 3. We readily observe that the PPH algorithm (Figure 3(d)) essentially avoids the Gibbs-like phenomenon that occurs with LIN4 (Figure 3(b)), and does not create artifacts of the type observed in ENO4 (Figure 3(c)).

This example clearly shows that ENO prediction techniques should not be applied in the standard two-dimensional extension (42) (see also [**1**], [**2**]). The artifacts observed in Figure 3(c) are a clear sign of instability, which is accentuated when ε is larger (not shown, see [**19**]) and also by the addition of texture, as we shall see in our next set of experiments (Figure 4). Numerical values of the compression ratio and the errors $\|A^L - \hat{A}^L\|_{l_p}$, $p = 1, 2, \infty$, for this particular experiment are compiled in Table 2. We see that the PPH exhibits the best relation

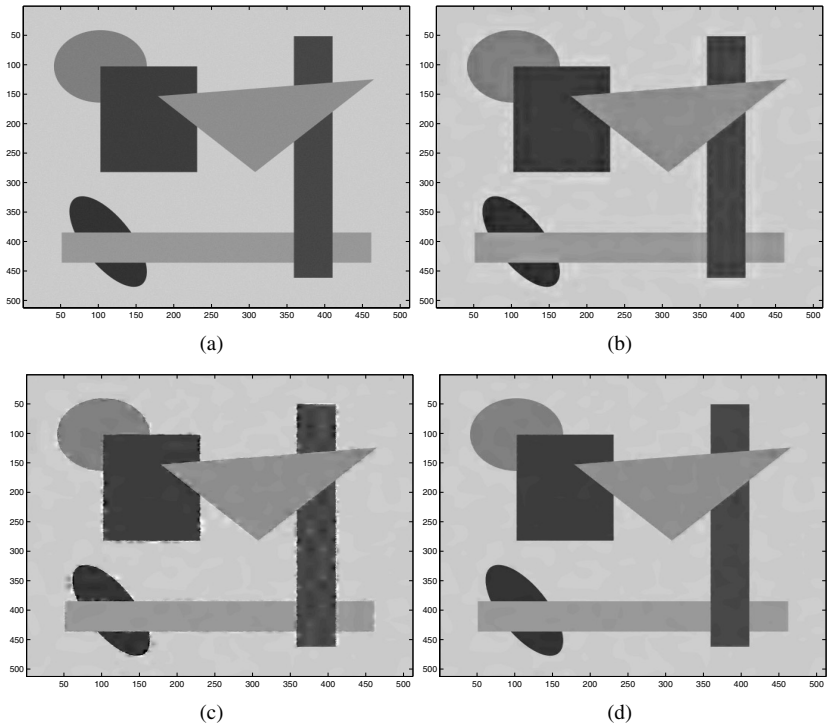

Fig. 4. (a) Geometric image with white noise, (b) LIN4, (c) ENO4, and (d) PPH, $L = 4$, $\varepsilon = 10$, noise level ≤ 5.

between r_c and the image quality, measured in any of the norms considered. The better image quality obtained by PPH can also be visually appreciated in Figure 3.

To study the effect of noise and texture on the properties of these algorithms, the geometric image is blurred with white noise of the l_∞ norm smaller than 5. We display the results obtained after applying the three algorithms, with the same parameters as in the previous case, in Figure 4 and in Table 3. As expected, the behavior of ENO4 with respect to the numerical artifacts is considerably worse, see Figure 4(c). Note also that the diffusion effect characteristic of LIN4 is now less regular and more noticeable, see Figure 4(b). On the other hand, when using the PPH algorithm the visual quality of the reconstructed image is essentially the same as that of the image without noise.

To better understand the effect of texture, we display in Figure 5 the full multiresolution representation corresponding to the images in Figure 4, that is, the coarsest resolution level A^0 together with the three types of interpolation errors $\{\Delta_i^k\}_{i=1}^3$ for $k = 1, 2, 3, 4$. White points correspond to nonzero coefficients after thresholding, i.e., significant details.

It can be seen that the effect of the texture is more noticeable in the errors corresponding to odd–odd locations, Δ_1^k. Looking at Figure 5 it can be observed

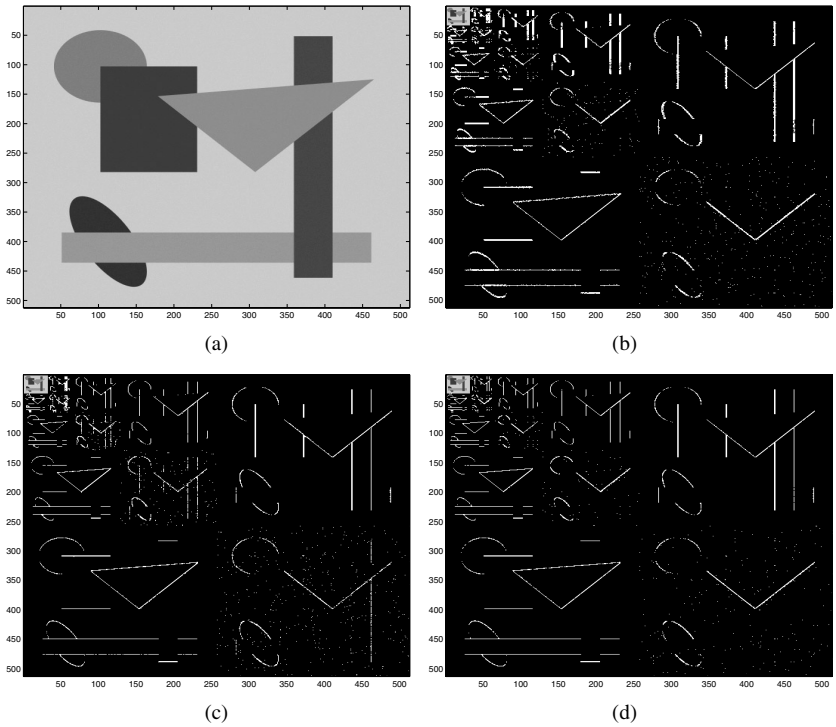

Fig. 5. (a) Geometric image with noise, (b) LIN4, (c) ENO4, and (d) PPH, $L = 4$, $\varepsilon = 5$, noise ≤ 4.

Table 2. Geometric image: Number of nonzero coefficients, compression ratio, l_∞, l_1, and l_2 norm of compression error, number of resolution levels $L = 4$.

$\varepsilon = 10$	LIN4	ENO	PPH
nnz	4701	4566	4644
r_c	$1.79e-02$	$1.74e-02$	$1.77e-02$
l_1	2.38	1.24	0.16
l_∞	30.86	88.83	21.26
l_2	4.39	4.98	1.00

Table 3. Geometric image with noise: Number of nonzero coefficients, compression ratio, l_∞, l_1, and l_2 norm of compression error, number of resolution levels $L = 4$.

$\varepsilon = 10$, noise ≤ 5	LIN4	ENO	PPH
nnz	5163	4846	4615
r_c	$1.97e-02$	$1.85e-02$	$1.76e-02$
l_1	2.91	2.77	1.61
l_∞	29.73	106.63	32.05
l_2	4.17	5.80	2.15

Fig. 6. Cameraman image.

that the area of white points is significantly smaller for the PPH. It seems, thus, that this algorithm is less influenced by the additional texture, keeping a smaller number of large details while retaining a similar overall quality in the reconstructed image. This can also be seen in Table 3.

Our next test concerns the cameraman image, displayed in Figure 6. This is an example of a real image where the geometrical features are dominant.

For this numerical test $J_L = 256$ and we consider $L = 4$ and $\varepsilon = 10$. A zoom of the reconstructed images on an edge-dominated region is displayed in Figure 7. As in the previous cases, the PPH algorithm leads to a reconstructed image free of numerical artifacts or blurred regions. The numerical values in Table 4 are also consistent with our observations, and the PPH leads to the best relation between r_c and quality of the reconstructed image.

For a real image with large texture regions such as the Lena image displayed in Figure 8, the behavior of the PPH algorithm is consistent with the observations made in the previous tests. The PPH algorithm achieves a better visual reconstruction of edge regions, while being comparable to LIN4 in texture regions. ENO4 without error control strategies is clearly out of the question for such images [**1**], [**2**].

Table 4. Cameraman image ($J_L = 256$): Number of nonzero coefficients, compression ratio, l_∞, l_1, and l_2 norms of compression error.

$\varepsilon = 10$	LIN4	ENO	PPH
nnz	12580	12467	12100
r_c	$1.91e-01$	$1.90e-01$	$1.84e-01$
l_1	3.82	4.72	3.25
l_∞	31.30	158.90	29.93
l_2	5.23	8.34	4.56

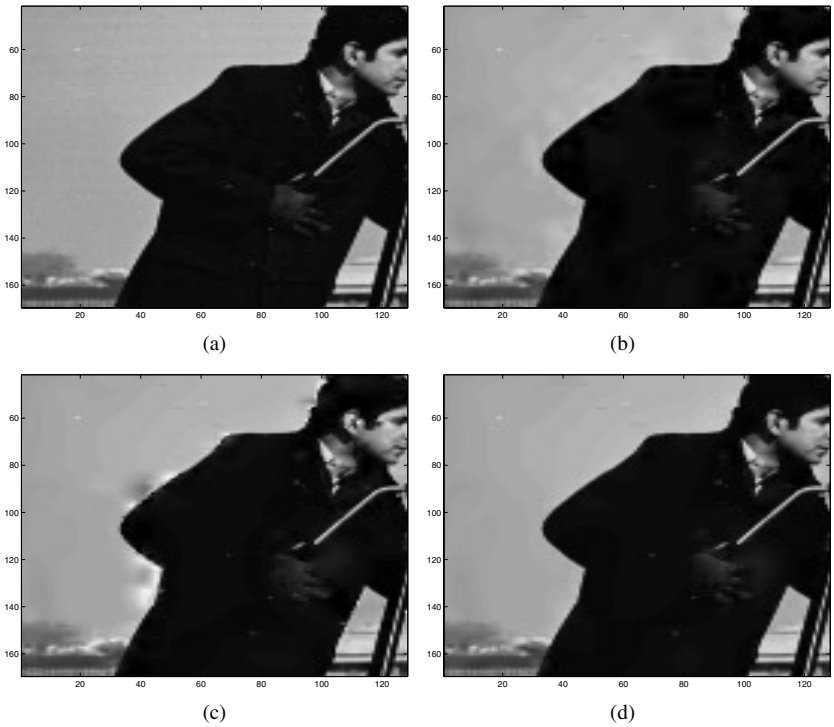

Fig. 7. (a) Original, (b) LIN4, (c) ENO4, and (d) PPH, $L = 4$, $\varepsilon = 10$.

We carry out a comparative study of the relation r_c versus image quality for the three schemes in the four test images using the PSNR (Peak Signal to Noise Ratio) quality image indicator [**18**]. We recall that for an 8 bit image,

$$PSNR = 20 \log_{10} \left(\frac{255}{\|A^L - \hat{A}^L\|_{l_2}} \right).$$

In Figures 9–12 the ratios $r_c^{\text{LIN4}}/r_c^{\text{PPH}}$ and $r_c^{\text{ENO4}}/r_c^{\text{PPH}}$ are plotted versus the PSNR. It can be observed that for a given level of quality, specified by the PSNR, the compression attained by PPH is higher than both LIN4 and ENO4, since both ratios are consistently above 1.

6. Conclusion

In this paper, a new fully nonlinear reconstruction operator in Harten's multiresolution framework has been presented. The corresponding nonlinear subdivision algorithm has been analyzed in terms of convergence, smoothness, and stability.

Fig. 8. (a) Original Lena image, (b) LIN4, and (c) PPH, $L = 4$, $\varepsilon = 15$.

The properties of the nonlinear subdivision scheme turn out to be crucial in proving the stability of the associated nonlinear multiresolution transform [**4**].

Using a tensor product strategy, applications to image compression have been performed. Edge resolution, robustness with regard to texture or noise, accuracy, and compression rate have been investigated. The numerical tests confirm that, as

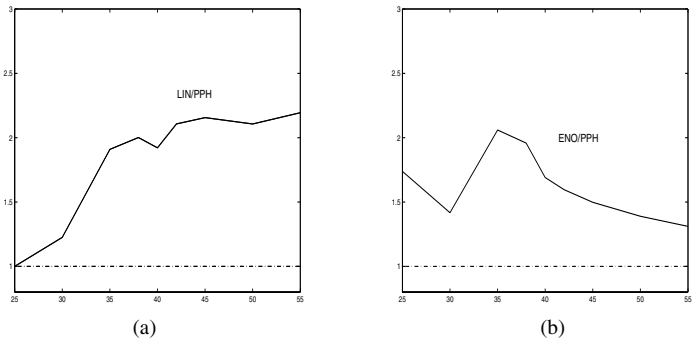

Fig. 9. Geometric image, (a) $r_c{}^{\mathrm{LIN}}/r_c{}^{\mathrm{PPH}}$ vs PSNR, and (b) $r_c^{\mathrm{ENO}}/r_c^{\mathrm{PPH}}$ vs PSNR, $L = 4$.

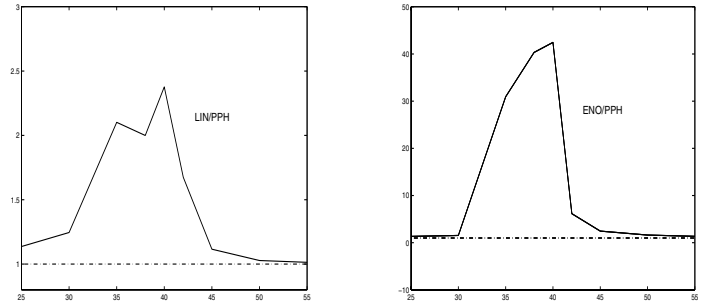

(a) (b)

Fig. 10. Geometric image with noise, (a) $r_c^{\text{LIN}}/r_c^{\text{PPH}}$ vs PSNR, and (b) $r_c^{\text{ENO}}/r_c^{\text{PPH}}$ vs PSNR, $L = 4$.

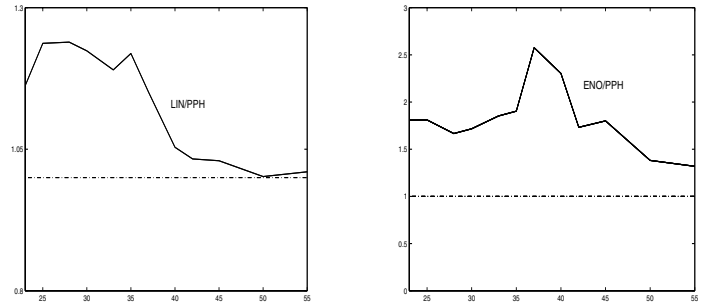

(a) (b)

Fig. 11. Cameraman image, (a) $\frac{r_c^{LIN}}{r_c^{PPH}}$ vs PSNR, (b) $r_c^{\text{ENO}}/r_c^{\text{PPH}}$ vs PSNR, $L = 4$.

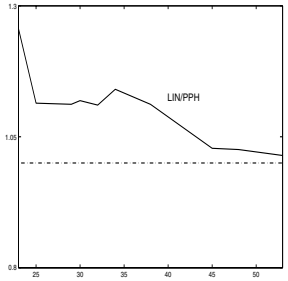

Fig. 12. Lena image, $r_c^{\text{LIN}}/r_c^{\text{PPH}}$ vs PSNR, $L = 4$.

proven in [**4**], the PPH multiresolution transform is a stable nonlinear algorithm that can be used for compression purposes. This should be contrasted with the well-known ENO multiresolution transforms, whose stability can only be ensured by implementing them with an Error Control strategy, as specified in [**1**], [**2**].

Using the *primitive function* [**13**] technique, the PPH interpolatory reconstruction described in this paper can be adapted to the cell-average framework, that is more suitable for image processing. This is currently work in progress.

Finally, one should mention that in our calculations the CPU time related to the PPH scheme remains, up to 4%, equivalent to the CPU time associated to the linear scheme.

Acknowledgment

Research partially supported by European network "Breaking complexity" # HPRN-CT-2002-00286. The research of Sergio Amat was supported in part by the Spanish grants MTM2004-07114 and 00675/PI/04.

References

[1] S. Amat, F. Aràndiga, A. Cohen, and R. Donat, Tensor product multiresolution analysis with error control for compact image representation, *Signal Process*. **82**(4) (2002), 587–608.

[2] S. Amat, F. Aràndiga, A. Cohen, R. Donat, G. García, and M. von Oehsen, Data compression with ENO schemes: A case study. *Appl. Comput. Harmon. Anal*. **11** (2001), 273–288.

[3] S. Amat, S. Busquier, and V. F. Candela, A polynomial approach to the piecewise hyperbolic method, *Internat. J. Comput. Fluid Dynam*. **17**(3) (2003), 205–217.

[4] S. Amat and J. Liandrat, On the stability of the PPH nonlinear multiresolution, *Appl. Comput. Harmon. Anal*. **18** (2005) 198–206.

[5] F. Aràndiga and R. Donat, Nonlinear multi-scale decomposition: The approach of A. Harten, *Numer. Algorithms* **23** (2000) 175–216.

[6] F. Aràndiga, R. Donat, and A. Harten, Multiresolution based on weighted averages of the hat function I: Linear reconstruction operators, *SIAM J. Numer. Anal*. **36** (1999), 160–203.

[7] F. Aràndiga, R. Donat, and A. Harten, Multiresolution based on weighted averages of the hat function II: Nonlinear reconstruction operators, *SIAM J. Sci. Comput*. **20**(3) (1999), 1053–1099.

[8] A. Cohen, N. Dyn, and B. Matei, Quasilinear subdivision schemes with applications to ENO interpolation, *Appl. Comput. Harmon. Anal*. **15** (2003), 89–116.

[9] G. Delauries and S. Dubuc, Symmetric iterative interpolation scheme, *Constr. Approx*. **5** (1989), 49–68.

[10] D. Donoho, Interpolating wavelet transforms, Preprint, Standford University, 1994.

[11] N. Dyn, Subdivision schemes in computer aided geometric design, in *Advances in Numerical Analysis*, *II. Subdivision Algorithms and Radial Functions*, W. A. Light (ed.), Oxford University Press, Oxford, pp. 36–104, Prentice-Hall, Englewood Cliffs, NJ, 1992.

[12] A. Harten, Discrete multiresolution analysis and generalized wavelets, *J. Appl. Numer. Math*. **12** (1993), 153–192.

[13] A. Harten, Multiresolution representation of data II, *SIAM J. Numer. Anal*. **33**(3) (1996), 1205–1256.

[14] A. Harten, S.J. Osher, B. Engquist, and S. R. Chakravarthy, Some results on uniformly high-order accurate essentially non-oscillatory schemes, *Appl. Numer. Math*. **2** (1987), 347–377.

[15] A. Harten, B. Engquist, S. J. Osher, and S. R. Chakravarthy, Uniformly high order accurate essentially non-oscillatory schemes III, *J. Comput. Phys*. **71** (1987), 231–303.
[16] A. Harten and Yad-Shalom, Fast multiresolution algorithms for matrix-vector multiplications, *SIAM J. Numer. Anal*. **31** (1994), 1191–1218.
[17] A. Marquina, Local piecewise hyperbolic reconstruction of numerical fluxes for nonlinear scalar conservation laws, *SIAM J. Sci. Comput*. **15**(4) (1994), 892–915.
[18] M. Rabbani and P. W. Jones, *Digital Image Compression Techniques*. *Tutorial Text*, Society of Photo-Optical Instrumentation Engineers (SPIE), TT07, 1991.
[19] J. C. Trillo, Multirresolución no lineal y Aplicaciones, PhD thesis, University of Valencia, Spain, 2005.